Study of Thallium, Lead, and Bismuth Nuclei Produced in the Bombardment of Gold with 380-Mev Protons*

ALBERT E. METZGER† AND J. M. MILLER
Department of Chemistry, Columbia University, New York, New York
(Received October 30, 1958)

Gold has been bombarded by the 380-Mev proton beam of the Nevis Cyclotron in a study of secondary reactions. Secondary reactions produce nuclei with charges greater than that of a target nucleus by means of an intermediate fragment emitted from one target nucleus and absorbed in a second. The increase in atomic number permits isolation of the effect by chemical separation.

Thallium, lead, and bismuth fractions were separated from irradiated gold bars and carefully purified. The radioactive decay of these samples was followed with a NaI(Tl) crystal scintillation counter. Nuclei produced by secondary reactions were detected for all three elements, the yields decreasing rapidly with increasing atomic number. From the secondary reaction yields of thallium and lead isotopes, it has been possible to calculate the upper portion of the energy distribution of the respective intermediate alpha and lithium fragments. This provides a comprehensive picture of a secondary reaction and demonstrates (1) that the yield of secondary particles is a rapidly increasing function of the bombardment energy for a given target nucleus, (2) that the energy distribution of the secondary fragment possesses an appreciable high-energy tail, and, (3) that secondary reactions can be treated in terms of conventional nuclear reaction theory.

I. INTRODUCTION

THE production of radioactive nuclides with atomic numbers two or three greater than that of the target has been observed in high-energy proton irradiations.[1–3] While it is possible to form them in the interactions between the primary protons and the target nuclei,[4] it is far more likely that these products are produced in nuclear reactions between target nuclei and secondary helium or lithium particles which have been produced within the target by the inelastic interactions of the incident high-energy protons.

Of the several studies of secondary reactions in medium-weight elements that have been reported,[1–3] the most detailed is that of Marquez and Perlman[3] who investigated the production of iodine in the proton bombardment of tin. To explain the surprisingly large yield of iodine which they found, it is necessary to postulate either that the cross section for forming lithium fragments with reasonable energies (about 30 Mev) is of the order of a barn, or that lithium fragments formed with a reasonable cross section (about 0.05 barn) possess an initial kinetic energy of the order of 100 Mev.

In the investigation of secondary reactions reported here, the choice of target, gold, presents two important advantages: the high atomic number lessens the difficulties caused by impurities in the target, and the fact that gold is monoisotopic greatly increases the information that may be derived from this kind of experiment. Since the apparent cross section for the production of a secondary product depends upon the differential cross section for the production of secondary fragments in a given energy interval and upon the probability that a secondary fragment of a given initial energy will participate in a nuclear reaction before being brought to rest by electromagnetic interactions, a monoisotopic target makes it possible to estimate the energy spectrum of the alpha and lithium fragments produced.

II. EXPERIMENTAL

A. Target Purity

The gold used in this investigation was obtained from two sources: Handy and Harman, Inc. (commercially rated as 99.99% pure), and Johnson-Matthey and Company (commercially rated as 99.999% pure). Since the anticipated yield of secondary products varied from very low to nonexistent, it was necessary to preclude the possibility that any product of a secondary reaction is formed from impurities in the gold via a spallation reaction. Therefore, thallium, bismuth, and lead were individually separated from typical gold targets by precipitation with a nonisotopic carrier. The first two elements were assayed by neutron activation; lead, which possesses a low thermal neutron cross section, was assayed colorimetrically with dithizone.[5] The results showed that the commercial gold contained from one-half to one ppm of lead and a fifth to one ppm of bismuth. The same series of analyses demonstrated that by repeated scavenging, the bulk of these impurities could be removed from gold. Accordingly,

* Supported in part by the U. S. Atomic Energy Commission and by the Office of Naval Research.

† Submitted in partial fulfillment of the requirements for the degree of Doctor of Philosophy in the Faculty of Pure Science, Columbia University.

[1] Batzel, Miller, and Seaborg, Phys. Rev. **84**, 671 (1951).

[2] A. Turkevich and N. Sugarman, Phys. Rev. **94**, 728 (1954).

[3] L. Marquez and I. Perlman, Phys. Rev. **81**, 953 (1951).

[4] A reaction involving the emission of π^- mesons could be considered an example of this statement. See, for example, Bonner, Friedlander, Pepkowitz, and Perlman, Phys. Rev. **71**, 511 (1947). The cross section for multiple π^- meson emission without a further breakup of the excited nucleus is negligible for irradiations with about 400-Mev protons.

[5] E. B. Sandell, *Colorimetric Determination of Traces of Metals* (Interscience Publishers, Inc., New York, 1950).

samples were so treated prior to two cyclotron irradiations, and the contribution of spallation reactions to the products of interest was greatly reduced.

B. Irradiations

Proton bombardments were performed in Columbia University's Nevis Synchro-Cyclotron at a radius corresponding to an energy of 380 Mev. Three different elements, gold, lead, and bismuth, served alternately as targets. Gold, the primary material, was irradiated in three forms: a commercial bar 2 cm×2 mm×2 mm; a powder which, following the preliminary chemical treatment mentioned in the preceding section, was carefully washed, dried, and wrapped in 2-mil aluminum foil; and as a foil 0.05 mm in thickness. The foils were bombarded in pairs, with each gold foil sandwiched between a set of three 2-mil aluminum foils. The stacked foil irradiations provided an absolute cross section for the production of the internal monitor (Au^{195}) through comparison with the known cross section for the $Al^{27}(p,3pn)Na^{24}$ reaction.

The bombardments of bismuth and lead targets were necessary because of the presence of the trace impurities of these elements in the gold. The lead and bismuth activities that were separated from lead and bismuth targets were compared with corresponding activities from gold bombardments. This was done in order to confirm the existence of the lead and bismuth formed from secondary reactions by observing differences in the gross decay curves. Subsequently, after measuring the cross sections for the production of lead and bismuth activities from lead and bismuth targets, it was possible to correct for the impurities found in the gold.

Bismuth was irradiated both as powdered bismuth oxychloride and as a 5-mil metallic foil. Five-mil lead foil was used for all lead irradiations. The internal monitor for the bismuth and lead irradiations was Bi^{205}. Its absolute cross section was measured in the same manner as described above for the gold monitor. All foils were obtained from J. D. McKay.

The bombardments of the gold bar and the gold powder targets were of two to three hours duration in order to maximize activities. All others were from 5–20 minutes in length.

C. Chemical Separations

The irradiated gold targets were dissolved in aqua regia. Five milligrams each of thallium, lead, and bismuth carriers were added and the solution was boiled to remove excess acid. Lead was precipitated as the sulfate, bismuth as the phosphate. Following these steps, the gold was carefully reduced with dilute hydrazine hydrate. The thallium in the supernatant solution was oxidized with nitric acid and extracted into diisopropyl ether.

The procedure for purifying the lead fraction consisted of an initial extraction into a dithizone solution in chloroform followed by alternate precipitations of lead sulfate and lead chromate. The sample was counted as the chromate. Bismuth was purified by repeated precipitation of bismuth phosphate and reduction of bismuth chloride by powdered nickel. Bismuth was counted as the phosphate. Thallium was purified by extraction into diisopropyl ether combined with the precipitation of thallous iodide. Thallium was counted as the iodide. Gold was cleaned by extraction into ethyl acetate and reduction by hydrazine hydrate. It was counted as the element. Holdback carriers were used at appropriate points in all procedures.

Chemical fractions from lead and bismuth targets were cleaned using the same methods outlined for gold, although there was some variation in the preliminary separation and fewer cleaning cycles were required.

D. Counting Techniques

The products of secondary reaction in gold are all expected to be on the neutron deficient side of stability and therefore to decay by electron capture. Scintillation detection presents a good method of recording such events when they occur in heavy elements. However, each electron capture will, in general, be accompanied by a spectrum of gamma rays, each with its own coefficient of internal conversion. For the scintillation counter to have the same efficiency for the detection of all disintegrations regardless of the number of gamma rays and the amount of internal conversion that may occur, it is necessary that the counter have an efficiency of 100%. If the efficiency is less than this, a different value of the efficiency, depending upon the individual decay scheme, would have to be applied to the counting rate of each nuclide in order to obtain even relative yields.

The counter, which has been designed to have a 4π geometry, consists of two Dumont 6292 phototubes, each fitted with a crystal of NaI(Tl). Tubes and crystals, after a light-tight wrapping with black electrical tape, have been enclosed in a brass box completely surrounded by two inches of lead shielding. The phototubes have separate high voltage supplies which are adjusted to provide an identical amplitude response from each phototube to signals of equal energy. Pulses from the phototubes are put through a common linear amplifier and pulse-height analyzer. All sample counting has been done with an infinite-energy channel width, and with discrimination at about 20 kev in order to eliminate low level noise. The pulse-height analyzer has also been used to identify the characteristic K x-rays of a particular element and thereby confirm the radiochemical purity of a sample. When the crystals are brought together to count a sample, the crystal assembly measures $1\frac{3}{4}$ inches in diameter and $1\frac{1}{2}$ inches in length. At the center is a well, $\frac{1}{2}$ inch in depth and $\frac{5}{8}$ of an inch in diameter, into which samples are placed for counting.

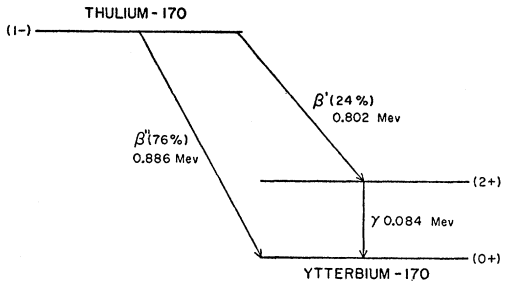

FIG. 1. Decay scheme of thulium-170.

The efficiency of the scintillation counter was determined by comparing the disintegration rate of a standard source with its measured counting rate in the scintillation counter. Thulium-170 was chosen as the standard since it emits gamma rays of 84 kev, an energy at which the unit efficiency is required, as well as an energetic beta particle. The decay scheme of this nuclide is simple and well known (see Fig. 1).[6]

The disintegration rate of the thulium standard was obtained by β-γ coincidence counting. If C is the recorded counting rate, d the disintegration rate, and f an over-all counting efficiency, we have:

for the gamma counter, $C_\gamma=0.24f_\gamma d$;
for the beta counter, $C_\beta=(0.24f_{\beta'}+0.76f_{\beta''})d$;

and for the number of coincidences, $C_{\beta\gamma}=0.24f_{\beta'}f_\gamma d$, so that

$$\frac{C_\beta C_\gamma}{C_{\beta\gamma}}=\frac{(0.24f_{\beta'}+0.76f_{\beta''})d}{f_{\beta'}}.$$

In order for $C_\beta C_\gamma/C_{\beta\gamma}$ to equal d, the counting efficiencies of the two betas must be equal. Since both transitions involve a spin change of one and a change in parity, and since the betas are not more than 10% apart in energy (0.886 Mev and 0.802 Mev), this equality should be a valid approximation.

The 84-kev gamma ray counting rate of Tm^{170} in the 4-π counter was obtained from the pulse-height distribution by measuring the area beneath its photoelectric peak. The contribution of the beta particles to the gamma-ray photoelectric peak was estimated by determining the pulse-height distribution above the 84-kev peak and extrapolating down to the energy interval of the peak. This correction amounted to about 16% of the gamma peak counting rate. From the counting rate of the gamma ray and the value (0.026) given by Jaffe[7] for the probability of its emission in Tm^{170} decay, a value of the disintegration rate as measured by the scintillation counter was calculated. This result was within 1% of the disintegration rate of the standard obtained by coincidence counting. Based on this value we may expect any single decay which emits only one photon of energy between 20 and 100 kev to have a detection efficiency of $99_{-4}^{+1}\%$. The efficiency of the scintillation counter will approach 100% for those heavy nuclides whose decay is accompanied by a gamma cascade.

The radioactive samples are put into a form suitable for counting in the crystal "well" in the following way: After a desired chemical fraction from an irradiated target has been separated and purified, it is suction-filtered onto a disk of highly retentive filter paper in a funnel assembly designed to distribute the sample uniformly over an area less than $\frac{3}{8}$ of an inch in diameter. When thoroughly dried this filter paper is then covered on each side by a disk of cellophane and over each piece of cellophane is placed a piece of scotch tape. The scotch tape holds the sample firmly in place, and the cellophane separators allow the sample to be easily recovered for chemical analysis.

III. RESULTS

Secondary-reaction cross sections for the production of thallium and lead isotopes in a gold target are given in Table I. Each value has been corrected for the contribution resulting from the spallation of bismuth and lead impurities in the gold target. The average percentage corrections [(uncorr.−corr.)×100/uncorr.] are given in column 4 of Table I. The errors assigned to the measured cross sections are root-mean-square deviations from the mean of several determinations. The anomalously low value for the cross section Tl^{197} was also found in the spallation of lead and bismuth. If this discrepancy is not due to a systematic error in resolving the decay curves, the most reasonable explanation would seem to be the existence of an isomeric state which was not detected.

The purest gold samples used in this work produced bismuth fractions with gross decay rates less than half of the 4π counter background. Since the initial activity of bismuth samples whose final chemical purification

TABLE I. Secondary reaction cross sections from the bombardment of gold by 380-Mev protons.

Isotope	Cross section with standard deviation (in microbarns)	Relative yields	Average impurity correction (%)
Tl^{195}	13.6 ±0.9	145	<1
Tl^{196}	17 ±7	185	<1
Tl^{197}	1.71 ±0.27	18	<1
Tl^{198}	42 ±8	450	<1
Tl^{199}	22.5 ±4.7	240	<1
Tl^{200}	1.46 ±0.34	16	3
Tl^{201}	0.094 ±0.028	1	27
Tl^{202}	<0.0011±···	<0.01	···
Pb^{198}	0.089 ±0.006	3.0	25
Pb^{199}	0.131 ±0.040	4.4	13
Pb^{200}	0.097 ±0.006	3.2	19
Pb^{201}	0.030 ±0.008	1	43
Pb^{202}	0.006 ±0.008	0.2	47
Pb^{203}	0.002 ±0.002	0.07	87

[6] Graham, Wolfson, and Bell, Can. J. Phys. **30**, 459 (1952).
[7] H. Jaffe, University of California Radiation Laboratory Report UCRL-2537, 1954 (unpublished).

occurs 6–8 hours after the end of bombardment contains isotopes with half-lives of 14.5 days, 6.4 days, and 12 hours, as well as possible shorter components, no resolution could be effected. It was therefore necessary to deal directly with the entire decay curve. The contributions to the bismuth-from-gold decay curves due to either lead or bismuth impurities in the gold were calculated by employing Bi^{205} as a standard of reference. The ratios of gross bismuth-from-impurity activities to their end of bombardment Bi^{205} activity were tabulated at intervals of several hours. Multiplying the ratio at a time t_i by the Bi^{205} cross section and the measured impurity level gives the gross bismuth activity at the time t_i due to the presence of that impurity.

When the calculated gross impurity activities were subtracted from the total activity of the bismuth-from-gold sample, the remainder was to be attributed to secondary reactions. However, those samples of bismuth-from-gold that were considered most reliable from the standpoint of effective cleaning and identification of the x-ray peak, were found to contain between 10 and 25% less activity than expected from the impurities alone.

Contradictory qualitative evidence has been observed by comparing the gross decay curves of bismuth fractions from gold, lead, and bismuth targets, respectively, and noting that the low level bismuth-from-gold fractions decay more rapidly than either of the other two curves. This is what would be expected for a secondary reaction: an increase in the proportion of neutron-deficient species.

A quantitative estimate of the amount of secondary bismuth present in a bismuth-from-gold curve has been made on the basis of the preceding observation, by assuming that a sample counting rate at the low activity end of the decay curve is due wholly to activity arising from impurities. Only the longer lived isotopes, whatever their means of formation, will be expected to survive to this reference time (about 100 hours after the end of bombardment). Since these long-lived bismuth isotopes are Bi^{205} (14.5 days) and Bi^{206} (6.4 days), their production via a secondary reaction between $Au^{197}+Be^{8}$ or Be^{9} would require the subsequent evaporation of zero or one neutron. However, in view of the energy which these beryllium secondary fragments must have in order to penetrate the Coulomb barrier ($\sim$40 Mev), multiple neutron emission should occur in the great majority of cases, so that Bi^{205} and Bi^{206} are probably not formed in secondary reactions.

From the bismuth-from-bismuth and bismuth-from-lead decay curves, taken in proportion to the ratios of bismuth and lead impurities in the sample, we calculate what the activity should be 18 or 24 hours after the end of bombardment, based on the counting rate at the 100 hours reference point. The difference between this value and the actual counting rate 18 or 24 hours after the end of bombardment is ascribed to secondary activity. This net activity is extrapolated back to the end of bombardment with a 12-hour half-life. Twelve hours is used because it was the shortest half-life which could be observed 18 hours after the end of bombardment (Bi^{203}, $t_{\frac{1}{2}}=12$ hr and Bi^{204}, $t_{\frac{1}{2}}=12$ hr). The secondary reaction cross section found in this manner for the formation of Bi^{203} and Bi^{204} from gold was 0.0026 ± 0.0009 microbarn.

An estimate of the upper limit of the bismuth-from-gold cross section has been made by an analysis of possible errors. The errors considered were: (1) the error in measuring the level of impurities of lead and bismuth, (2) the error in measuring the cross section for Bi^{205} produced by lead and bismuth, and (3) the error in measuring the proton intensity of a given bombardment. The rms of these errors yielded 0.004 ± 0.001 microbarn as the probable upper limit of the cross section. This compares with a total cross section of 0.40 microbarn for all resolved lead isotopes produced by secondary reactions, and a total cross section of 98 microbarns for all resolved thallium isotopes produced by secondary reactions, an increase of roughly two orders of magnitude per unit charge increase of the intermediate fragment.

IV. DISCUSSION

A. Experimental Characteristics of Secondary Reactions

The following features clearly establish the fact that the cross sections listed in Table I represent secondary reactions, rather than spallation reactions:

(1) Both secondary reaction distributions peak, the thallium at $A=198$ and the lead at $A=199$; the spallation distributions do not peak at these mass numbers.

(2) The relative yields of the more neutron-abundant isotopes are much lower for the secondary reactions than for the spallation reactions. The isotope Tl^{202} was not detected in the secondary product distribution because its production by means of a doubly-charged intermediate fragment would require a particle with a mass greater than four, and on the basis of nuclear stability, such nuclides should comprise only a very small fraction of the helium isotopes produced.[8] The cross section of Tl^{201} will be small because, although the penetration of the monoisotopic gold nucleus ($A=197$) by an alpha particle results in a combined mass of 201, most of the secondary alpha particles which penetrate the Coulomb barrier do so with considerable energy and the chance that no subsequent

[8] It is possible to form Tl^{202} via a secondary reaction involving a lithium particle as the intermediate fragment followed by proton emission, but the cross section for such a process will be negligible for two reasons: (1) the total cross section for secondary reactions involving lithium fragments is very much lower than the total cross sections involving alpha fragments and (2) proton emission is highly unfavorable vis-à-vis neutron emission for heavy elements.

nucleon emission occurs is slight. An analogous situation in terms of lithium fragments is responsible for the decrease in the secondary reaction yield from Pb^{201} to Pb^{203}.

(3) The sharp drop in the total cross section of secondary reactions as we go from thallium to bismuth is due to a decrease in the secondary fragment yield as the atomic number of the fragment increases. This rate of change, about two orders of magnitude per unit charge increase in the secondary product, is much greater than can be accounted for by any distribution of impurities in the gold target.

(4) The purity of the gold targets used for the bombardments was not the same in all cases. The apparent cross section for a given isotope therefore varied, sometimes very widely, from bombardment to bombardment. After making the appropriate correction to each value of the apparent cross section, according to the level of the impurities which were present, the resultant cross sections not only remained finite, but showed much better agreement with each other than did the apparent cross sections.

B. Analysis of Secondary Reaction Parameters

The basic mechanism of a secondary reaction is straightforward, although certain details remain obscure. For the purposes of the treatment which follows, a secondary reaction will be divided into a three-stage process: (1) production of the secondary fragment in the course of an interaction between the incident particle and a target nucleus, (2) the collision of this fragment with a second target nucleus to form what will be referred to as a secondary compound-nucleus, and (3) the subsequent de-excitation of this secondary compound-nucleus. The cross sections presented in Table I represent the relative number of nuclei produced in a secondary reaction by intermediate fragments of a given atomic number. To see if these results are consistent with other available data, it is necessary to identify and evaluate the parameters that characterize each of the above stages.

In stage one we need to know the total cross section for production of the secondary fragment, σ_f, as well as the variation of this cross section with the fragment energy $\sigma_f(E)dE$.

Stage two, the formation of the secondary compound nucleus, requires a knowledge of the probability that a fragment will undergo a secondary reaction with a target nucleus. The cross section for the formation of secondary compound nuclei can be expressed as

$$\sigma_s=\int_0^\infty \sigma_f(E)P_c(E)dE, \tag{1}$$

where $P_c(E)$ is the probability that a fragment of initial energy E will interact with a target nucleus at some point in its range to give a secondary compound nucleus. This probability can be expressed as

$$P_c(E)=\int_0^E n\sigma_c(\epsilon)dr=\int_0^E n\pi R^2T(\epsilon)dr, \tag{2}$$

where n is the number of target nuclei per cubic centimeter; σ_c is the cross section for formation of a compound nucleus and is given by the product of the geometric cross section and a coefficient, $T(\epsilon)$, for penetration of the potential barrier; r is the distance travelled by the fragment. A relationship between energy and range will eliminate one of the variables and permit integration.

The first step in studying the de-excitation of the compound nucleus is to calculate the probability distribution of excitation energy deposited by the secondary fragment. This distribution can be obtained from the equation

$$P_x(U)=\int_U^\infty \sigma_f(E)P_t(E/U)dE \Big/ \sigma_f, \tag{3}$$

where $P_t(E/U)$ is the probability that a secondary fragment of initial energy E will introduce a quantity of excitation energy U (U includes the binding energy of the reaction) into the compound nucleus and $P_x(U)$ is the same probability taken over the entire secondary fragment energy distribution. The relationship between the probabilities $P_c(E)$ and $P_t(E/U)$ is given by the equation

$$P_c(E)=\int_0^E P_t(E/U)dU. \tag{4}$$

At this point it is necessary to introduce the reasonable assumption that proton emission is negligible in the de-excitation of these secondary compound nuclei. This assumption is based on the effect of the Coulomb barrier in inhibiting the emission of charged particles from heavy elements and has been borne out by experiments.[9] By the use of this assumption the process of de-excitation can be confined to the evaporation of neutrons. With the excitation energy distribution, it is possible to calculate the relative probabilities of emitting a given number of neutrons from the secondary compound-nucleus if we also know how the probability for the emission of a given number of neutrons varies with the excitation energy of the compound nucleus. The latter probability has been investigated by Jackson[10] from whose results we obtain the quantity $P_v^y(U)$, the probability of evaporating y neutrons from a nucleus having an excitation energy U. The relative number of secondary nuclei resulting from the emission of y neutrons from the excited compound nucleus will thus be given by

$$N_y=\int_0^\infty P_x(U)P_v^y(U)dU. \tag{5}$$

[9] Walter John, Jr., Phys. Rev. **103**, 704 (1956).
[10] J. D. Jackson, Can. J. Phys. **34**, 767 (1956).

It is evidently possible to reverse the order of steps in this treatment and, beginning with an isotopic distribution of secondary nuclei, to calculate an excitation probability function, $P_x(U)$, and consequently a secondary-fragment energy distribution, $\sigma_f(E)dE$. This has been done from the data for both sets of secondary products, thallium and lead, given in Table I. Details and results of this procedure will be given in the following section and some comparisons will be made with relevant data previously reported in the literature.

C. Application of Analysis to Experimental Results

The experimental results for thallium, with an interpolated value for Tl^{197}, were used to construct both the excitation probability function, $P_x(U)$, shown in Fig. 2 and the energy distribution of alpha particles shown in Fig. 3. Both computations were made by using numerical methods to solve the integral equations (5) and (3). The values of σ_c were obtained by interpolation from a table of capture cross sections given in Blatt and Weisskopf.[11] Ranges of the alpha particles in gold were obtained from a range-energy plot for alpha particles in lead[12] by making the appropriate corrections for mass, charge, and ionization potential.

Bailey[13] has directly measured the energy distribution of alpha particles produced in the bombardment of gold with 190-Mev protons. The two alpha particle energy distributions are compared in Fig. 3. Ratios of the two distributions, computed for a series of energies, demonstrate a tendency for the average energy of emission of the secondary fragment to shift to higher energies with increasing incident particle energy (see Table II). The curve derived from the experimental thallium distribution is cut off at about 27 Mev due

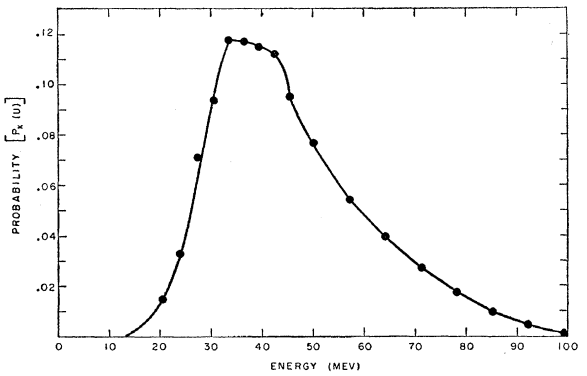

FIG. 2. Probability distribution of excitation energy for secondary thallium compound nuclei—from secondary yields.

[11] J. M. Blatt and V. F. Weisskopf, *Theoretical Nuclear Physics* (John Wiley and Sons, Inc., New York, 1952), pp. 352–353.
[12] Aron, Hoffman, and Williams, U. S. Atomic Energy Commission Report AECU-663, 1949 (unpublished).
[13] L. E. Bailey, University of California Radiation Laboratory Report UCRL-3334, 1956 (unpublished).

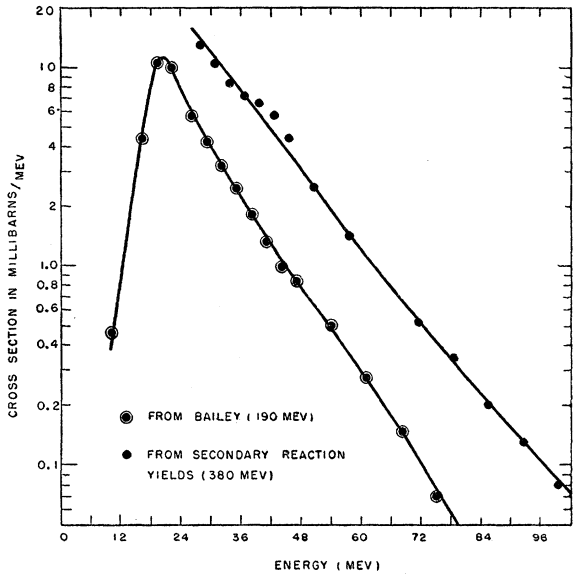

FIG. 3. Energy distributions of secondary alpha particles.

to the insensitivity in this experiment to lower energy alpha particles. This comes about because secondary fragments produced with an energy in the vicinity of, or lower than, the potential barrier, have a comparatively limited range in which to initiate a secondary reaction. The calculated energy distribution is therefore most reliable at the high energy end; this is in contrast to Bailey's distribution which is most dependable in a 20–30 Mev energy range centered near the Coulomb barrier because of the greater number of events measured in this interval.

The excitation energy probability distribution, $P_x(U)$, derived from Bailey's energy distribution for alpha particles, was obtained by numerical integration (see Fig. 4). Using this distribution in (5), it was possible to calculate secondary reaction yields of thallium isotopes. A comparison of the calculated values with the experimental results is given in Table III and shows reasonably good agreement. The maximum is at Tl^{198} in both cases. The percentage yields show that there is a definite shift towards the more neutron deficient species as the bombarding energy increases, as expected in view of the previous observation that the alpha energy distribution shifts towards higher energy with increasing proton energy. The total calcu-

TABLE II. Ratios of alpha particle energy distributions produced by 380-Mev and 190-Mev proton bombardment of gold (from Fig. 3).

Alpha particle energy (Mev)	Ratio
70	4.8
60	4.2
50	4.0
40	3.7
30	3.1

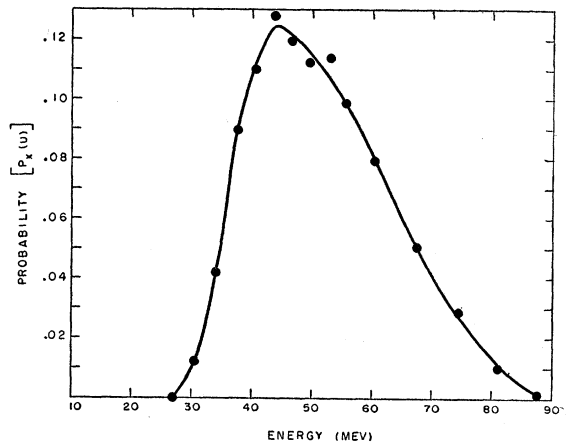

FIG. 4. Probability distribution of excitation energy for secondary thallium nuclei—from Bailey.

lated cross section for the production of thallium from gold due to 190-Mev protons is 21 microbarns, compared to 98 microbarns measured with 380-Mev protons.

A treatment of those secondary reactions which produce lead isotopes in a gold target is complicated by the fact that the secondary fragment may be any one of at least three lithium nuclei.[14] In order to use the isotopic distribution of lead to estimate the energy spectrum of the emitted lithium nuclei, it is necessary to know the relative yields of Li^6, Li^7, and Li^8. This information can be obtained from measurements by Deutsch of the relative amounts of light charged particles emitted in the high-energy (340 Mev) bombardment of various elements.[15] From his results for a gold target and the addition of the assumption that the energy distributions of these three nuclei are identical, ratios of 0.55:0.41:0.043 for Li^6:Li^7:Li^8 are obtained. After using these ratios in the estimation of N_y, it is possible to follow the same procedure that was described above for thallium in the computation of both an excitation energy probability function, $P_x(U)$, for secondary compound lead nuclei produced in the reaction of lithium particles with gold nuclei, and an energy distribution of lithium fragments produced in the initial interaction of high energy protons and gold. Rather than perform a detailed and difficult computation for the quantum mechanical penetration coefficient, $T(\epsilon)$, of gold nuclei by lithium particles, an approximation was made by analogy to the corresponding coefficients for alpha particles. The penetration coefficients for alpha particles were compared to those obtained from the classical function $(1-V/\epsilon)$ (where V is the potential barrier and ϵ is the particle energy) and the percentage difference was calculated. This percentage difference was used to correct $(1-V/\epsilon)$ for lithium particles (for identical values of V/ϵ) to give an estimate of the lithium-on-gold penetration coefficients. The ranges of lithium fragments in gold were computed from the corresponding ranges of alpha particles in lead[12] with corrections for mass, charge, and ionization potential of the gold target as well as for the mass and charge of the fragments themselves.

The distributions of $P_x(U)$ and $\sigma_f(E)$ for the production of lead in gold are shown in Fig. 5 and Fig. 6, respectively. The latter is cut off at the low-energy end for the same reason previously discussed for the calculated energy distribution of alpha particles. The cutoff is further above the Coulomb barrier for lithium particles than it is for alpha particles, which suggests that the actual yield of Pb^{201}, of Pb^{202}, or of both should be somewhat higher than those found experimentally, or that there should be a greater proportion of Li^6 in the secondary fragment ratio.

In the case of secondary reactions which produce bismuth, no detailed treatment could be made since the experimental data are so sketchy. We are therefore restricted to substituting the estimated bismuth secondary cross section (0.0026 microbarn) in a simpli-

TABLE III. Percentage yields of thallium isotopes produced by secondary reactions.

Atomic number	200	199	198	197	196	195	194
Calculated %	1	23	37	25	12	3.2	0.22
Experimental %	1	18	33	24[a]	14	10	···

[a] Interpolated.

[14] In the preceding treatment of thallium, all of the secondary fragments were assumed to be alpha particles. This is not true; He^3 is also produced, but according to measurements made by Deutsch contributes less than 4% to the total number of secondary helium particles.

[15] R. W. Deutsch, Phys. Rev. **97**, 1110 (1955).

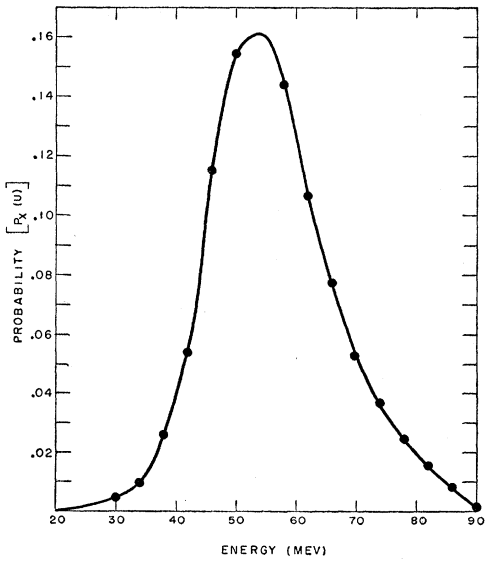

FIG. 5. Probability distribution of excitation energy for secondary compound lead nuclei.

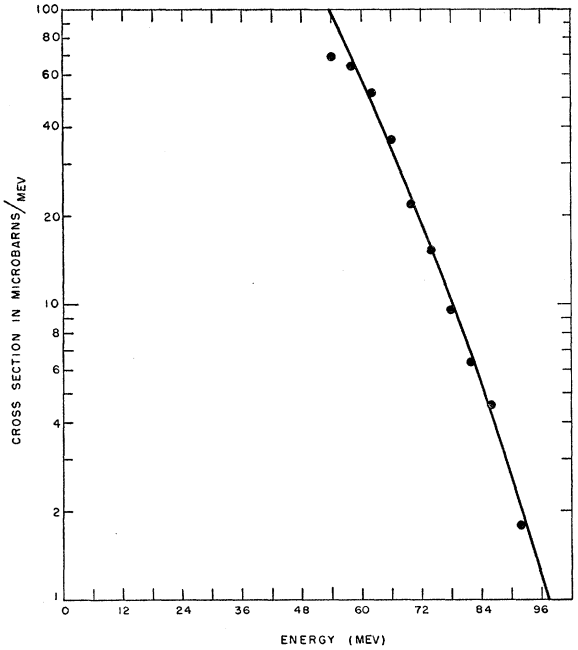

FIG. 6. Energy distribution of secondary lithium particles.

fied form of (1):

$$\sigma_f=\sigma_s/P_c(E)=\sigma_s\Big/\int_0^E n\pi R^2T(\epsilon)dr \qquad (1a)$$

in order to calculate a total cross section for the monoenergetic emission of beryllium fragments for a series of assumed energies, E. The results are shown in Table IV. Marquez and Perlman have measured the yield of beryllium seven fragments in the 335-Mev proton bombardment of gold to be 10^{-5} barn.[4] This corresponds to a monoenergetic emission energy of about 100 Mev, an unexpectedly high value. The contribution of beryllium fragments with mass numbers other than seven will lower the required emission energy. In addition, either too high a cross section for the production of bismuth in the gold target, or too low a cross section for the emission of beryllium particles could give rise to an error. Both measurements were handicapped by extremely low sample decay rates.

Table V presents a direct comparison between the data reported by Marquez and Perlman and the results of this investigation. For a given emission energy of lithium fragments, the cross section for lithium formation must be 30–50 times greater to produce the yield of iodine nuclei in a tin target measured by Marquez and Perlman, than to produce the yield of lead nuclei in a gold target measured in this experiment. The results of Deutsch for the relative numbers of secondary particles emitted from silver and gold contain no evidence that the total cross section for secondary fragment emission varies with the atomic number of the target.[15]

TABLE IV. Corresponding values of the calculated cross section and the effective emission energy of beryllium fragments produced in the 380-Mev proton bombardment of gold.

E(Mev)	49.6	52.5	60	70	97	129
σ_{Be}(barns)	10^{-3}	4×10^{-4}	10^{-4}	4×10^{-5}	10^{-5}	4×10^{-6}

Munir has measured the cross section for the production of Li^8 in the 950-Mev proton bombardment of silver and bromine (using emulsion plates) to be 1.1 ± 0.3 millibarns.[16] If we assume that this cross section is valid at about 350 Mev, and multiply it by the ratio of Li^6 plus Li^7 to Li^8 computed from their relative yields, a cross section for lithium emission of 26 millibarns is obtained. This corresponds to a lithium emission energy of more than 100 Mev in order to produce the measured cross section of iodine in tin, but requires less than 43 Mev to account for the cross section of lead in gold. Even if the total cross section for lithium production is reduced by as much as a factor of five, as an estimate of the decrease in the Li^8 cross section for the change in proton energy from 950 Mev to 380 Mev, the effective emission energy for lithium particles in gold is still well within the energy distribution of Fig. 6.

TABLE V. Corresponding values of the calculated cross section and the effective emission energy of lithium fragments produced.

A. 335-Mev proton bombardment of tin[a]						
E(Mev)	36	40	50	80	120	200
σ_{Li}(barns)	3.0	1.2	0.3	5×10^{-2}	2×10^{-2}	5×10^{-3}
B. 380-Mev proton bombardment of gold						
E(Mev)	38.2	40.2	47	54.5	76.5	104	182
σ_{Li}(barns)	0.1	0.04	0.01	4×10^{-3}	10^{-3}	4×10^{-4}	10^{-4}

[a] See reference 3.

In conclusion, the results of these three secondary reactions have shown that:

(1) In contrast to the findings of Marquez and Perlman, there is no evidence to support either an anomalously large cross section for the production of secondary fragments or of an extremely high average energy of emission.

(2) The yield of secondary particles is a rapidly increasing function of the bombarding energy for a given target nucleus.

(3) The experimental isotopic distribution of secondary nuclei requires that the energy distribution of secondary fragments possess a substantial high-energy tail.

(4) The entire secondary reaction can be treated in a straightforward manner by ordinary nuclear reaction theory.

[16] B. A. Munir, Phil. Mag. **1**, 355 (1956).

ACKNOWLEDGMENTS

We wish to express our appreciation to Dr. Warren Goodell for his kind cooperation, and to members of the Nevis cyclotron operating staff for performing the proton irradiations. We are deeply indebted to Dr. Daniel H. Greenberg, Dr. Sheldon Kaufman, and Mr. Edwin T. Hunter for their assistance in the laboratory and for many profitable discussions. Thanks are also due to the U. S. Atomic Energy Commission for their support of this research and to Dr. Frank Spedding, who supplied the thulium with which to measure the efficiency of the scintillation counter.

PHYSICAL REVIEW VOLUME 113, NUMBER 4 FEBRUARY 15, 1959

Photoproduction of Charged π Mesons from Nuclei*

JOHN R. WATERS†
Cornell University, Ithaca, New York

(Received October 20, 1958)

The γ-ray beam from the Cornell synchrotron was used to investigate the photoproduction of low-energy charged π mesons from several nuclei at 35° to the beam direction. Maximum photon energies used were 800 Mev and 1 Bev. The yields of 40 and 80 Mev π^+ and 40 Mev π mesons were observed with a detection system whose aperture was known absolutely. It was found that in some cases the meson yields were proportional to the atomic number, A, of the target rather than the more usual $A^{\frac{2}{3}}$. The data are compared with the predictions of an optical model of the nucleus. The deviations observed can be partially explained in terms of the inelastic scattering of high-energy mesons and of multiple meson production. An excitation function was measured for 80 Mev π^+ mesons from carbon by varying the machine energy; this indicated the presence of an appreciable number of multiply produced mesons.

I. INTRODUCTION

THE photoproduction of π mesons from complex nuclei has been studied with a view to investigating the behavior of the mesons inside nuclear matter, rather than to learn more about the basic photoproduction process. Previous workers[1–7] have found a meson yield which varies as $A^{\frac{2}{3}}$, where A is the atomic number of the nucleus. This result is usually explained in terms of an optical model in which the mesons are uniformly produced in the nuclear matter, but their interaction mean free path is so short that only those from the surface can escape to be detected. It is found that the effect of the Coulomb barrier is appreciable, especially for the lower energy mesons and the heavier nuclei.[8,9] The results of meson scattering experiments[10] confirm that the interaction mean free path is short; for example, it is about a meson Compton wavelength at 60 Mev. In general the predictions of the optical model agree with the several experiments performed with bremsstrahlung of energy up to 550 Mev.

In this report we extend the measurements of low-energy meson yields from bremsstrahlung of up to 1 Bev for a range of nuclei. It is found that there are significant differences in the yield as compared with the lower energy data. In some cases the meson yield appears to be proportional to A and in others it is intermediate between A and $A^{\frac{2}{3}}$. Measurements were also made of the ratio of the yields of negative to positive mesons using a detection system which was equally efficient for both. Since the aperture of the detection system was known, the meson cross sections reported are known absolutely.

II. EXPERIMENTAL METHOD

The arrangement of the apparatus is shown in Fig. 1. The gamma-ray beam from the Cornell synchrotron was collimated, struck the meson producing target and was absorbed in the beam monitoring ionization chamber. A magnet selected those mesons emitted at 35° to the beam direction and having the required momenta, and caused them to enter the counter telescope which was shielded from direct radiation by several inches of lead.

The magnet was that used in a previous experiment[11]

* Supported by the joint program of the Office of Naval Research and the U. S. Atomic Energy Commission.

† Now at the United Kingdom Atomic Energy Research Establishment, Harwell, England. This paper is based on a thesis submitted to the Graduate School of Cornell University in partial fulfillment of the requirements for a Ph.D. degree.

[1] R. M. Littauer and D. Walker, Phys. Rev. **86**, 838 (1952).
[2] Imhof, Perez-Mendez, and Easterday, Phys. Rev. **100**, 1798 (A) (1955).
[3] W. L. Imhof, University of California Radiation Laboratory Report UCRL-3383 (unpublished).
[4] Imhof, Knapp, and Perez-Mendez, Bull. Am. Phys. Soc. Ser. II, **1**, 173 (1956).
[5] Motz, Crowe, and Friedman, Phys. Rev. **98**, 268 (A) (1955).
[6] Motz, Crowe, and Friedman, Phys. Rev. **99**, 673 (A) (1955).
[7] Williams, Crowe, and Friedman, Phys. Rev. **105**, 1840 (1957).
[8] W. R. Hogg and D. Sinclair, Phil. Mag. **1**, 466 (1956).
[9] J. G. Rutherglen, *Proceedings of the Sixth Annual Rochester Conference on High-Energy Nuclear Physics* (Interscience Publishers, Inc., New York, 1956), IX-50.
[10] D. H. Stork, Phys. Rev. **93**, 868 (1954).
[11] Jenkins, Luckey, Palfrey, and Wilson, Phys. Rev. **95**, 179 (1954).